Study of the order–disorder transition and martensitic transformation in a Cu–Al–Be alloy by EELS

J.H. Hernández, M.T. Ochoa, H. Flores-Zúñiga, F. Espinosa-Magaña, D. Ríos-Jara

Abstract

Changes in 3d states occupancy associated with order–disorder transition and martensitic transformation in a Cu–Al–Be alloy was investigated by electron energy loss spectroscopy (EELS) in both high energy and low energy loss regions. From the high energy loss region, the Cu $L_{2,3}$ white-line intensities, which reflect the unoccupied density of states in 3d bands, was measured for three states of the alloy: disordered austenite, ordered austenite and martensite. It was found that the white-line intensity remains the same during order–disorder transition but appears slightly smaller in martensite, indicating that some electrons left Cu 3d bands or some hybridization took place during phase transformation. From the low energy loss region, the optical joint density of states (OJDS) was obtained by Kramers–Kronig analysis. As maxima observed in the OJDS spectra are assigned to interband transitions, these spectra can be used to probe changes in the electronic band structure. The analysis shows that during the martensitic transformation, the peaks positions and relative intensities in the OJDS spectra undergoes noticeable changes, which are associated with interband transitions.

Keywords: EELS; Electronic structure; Cu–Al–Be alloy; Martensitic transformation.

Introduction

Martensitic transformation has been observed in several materials and alloys, particularly in noble-metal-based alloys. From these, Cu-based alloys have received in recent decades considerable attention because of their shape memory properties [1,2]. These alloys are characterized by a high temperature stable β-phase with a disordered bcc-type unit cell (A2). β-phase presents different types of chemical ordering [3], on cooling below the eutectoid temperature (~450 °C) giving place to a bcc B2-ordered phase, having a CsCl type crystalline structure. Moreover, B2 can evolve to a DO_3 ordered-structure (β_1-phase) at slightly lower temperatures. For the $Cu_{0.75}Al0.22Be_{0.03}$ alloy studied in this work, DO_3 is the more likely from a stoichiometrical point of view, since it means near 3:1 ratio between Cu and Al atoms, with Be atoms substituting a small proportion of Cu atoms. In this case, the A2-structure undergoes a direct transition to DO_3, which on further cooling transforms to the martensitic β'-phase with an orthorhombic 18R-type structure [4]. This transformation is responsible for the shape memory effect. The transformation temperature depends on the composition, and very often small quantities of a third element are used to obtain a very broad range of transformation temperatures, which is the case of Be in the Cu–Al–Be alloy.

Even though it is recognized that the electronic structure plays an important role in the study of phase transformations, these kind of studies are not a common issue in the literature. In this article we studied the changes in electronic structure associated with a diffusive order–disorder transition, followed by a nondiffusive martensitic transformation in a Cu–Al–Be alloy, where the addition of small amounts of Be to the

stoichiometric Cu_3Al does not modify significantly the composition and temperature of the eutectoid point in the equilibrium phase diagram.

Theory

Electron energy loss spectroscopy (EELS) is a powerful analytical technique that can be utilized to obtain information on the structure, bonding and electronic properties of a material [5–11]. The interactions of fast electrons with the specimen result in excitations of electrons into unoccupied energy levels in the conduction band as well as collective excitations of valence electrons. When a spectrum is obtained by analyzing the energy lost by the incident electrons, the region up to an energy loss of ~50 eV is dominated by collective excitations of valence electrons (plasmon) and by interband transitions. At higher energy losses ionization edges occur due to excitation of core electrons into the conduction band.

The excitation of atomic inner shells by high energy electrons provides a method for studying the unoccupied conduction states in a solid. These core-level processes are mostly sensitive to final states since the initial states have narrow energy widths. Besides the well-defined ionization edges there is a fine structure superposed on the edge and extending up to about 50 eV from the edge onset, which is associated with the density of unoccupied states in the conduction band, known as the energy loss near edge structure (ELNES).

In case of 3d transition metals as well as their alloys, $L_{2,3}$ edges of EELS are characterized by two sharp peaks, termed as “white lines”. Because the predominance of dipole transitions, these white lines originate from excitations of $2p_{1/2}$ and $2p_{3/2}$ core

electrons to unoccupied d-like states near the Fermi level. The white-line intensities reflect the unoccupied 3d density of states (DOS). Data on the occupancies of 3d and 4d states can clarify many issues fundamental to electronic theories of transition metal alloys, including phase transformations.

The 3d and 4d occupations of transition metals have been studied systematically by several authors [12–20]. Pearson et al. [12] have attempted to relate the sum of the L_3 and L_2 white-line intensities to the occupancies of the corresponding outer d states. The experimental studies on the white lines from $L_{2,3}$ EELS spectra for elemental metals of the 3d transition series found that the normalized intensities of these white lines decreased nearly linearly with increasing d-state occupancy across the series. The normalized white-line intensity was defined as the integrated intensity of the L_2 and L_3 white lines divided by the integrated intensity in a normalization window 50 eV in width beginning 50 eV past the L_3 edge onset. When the normalized white-line intensities for the 3d metals were divided by appropriate matrix-element correction factors, which were calculated for each atomic species, a linear correlation with 3d occupancy was obtained with a fit given by:

$$I'_{3d} = 10.8(1 - 0.1n_{3d}) \qquad (1)$$

where I'_{3d} is the normalized white-line intensity divided by the appropriate matrix-element correction factor and n3d is the 3d occupancy in electrons/atom. The above correlation between the normalized white-line intensity and 3d occupancy (electrons/atom) is useful for determining changes in outer d stat occupancy upon

alloying and solid-state phase transformations if the corresponding changes in the normalized white-line intensity are observed.

On the other hand, the low loss region in an energy loss spectrum (<50 eV) contains information about excitations of outer shell electrons and the electronic structure of the material which determines its optical properties. The excitations of valence electrons are dominated by collective excitations (plasmons) and also by single electron interband transitions. Interband transitions originate from the excitation of electrons in the valence bands to empty states in the conduction bands, so these can be identified as transitions in a band structure model.

From the dielectric theory, it is possible to relate the experimental single scattering distribution S(E), to the energy loss function Im (-1/ε), by [5]:

$$S(E) = \frac{I_0 t}{\pi a_0 m_0 v^2} \operatorname{Im}\left[-\frac{1}{\varepsilon(q, E)}\right] \ln\left[1 + \left(\frac{\beta}{\theta_E}\right)^2\right] \qquad (2)$$

Where $\varepsilon(q,E) = \varepsilon_1 + i\varepsilon_2$ is the complex dielectric function at energy loss E and momentum transfer q, a_0 the Bohr radius, m_0 the electron rest mass, v the electron beam velocity, θ the scattering angle and $\theta_E = E/(\gamma m0v^2)$ the characteristic scattering angle, γ the relativistic factor, I0 the zero loss intensity, t the specimen thickness and β is the collection semi-angle.

As peak positions in the energy loss spectrum at low energy losses are strongly influenced by the volume plasmon and the positions of other excitations, the energy loss spectrum cannot be directly associated with interband transitions. However, the imaginary part of the dielectric function $\varepsilon_2(E)$, can be associated with interband

transitions. In turn the real and imaginary parts of the dielectric function can be obtained from the energy loss function through Kramers–Kronig analysis [5].

To relate experimental results from EELS with the band structure density of states (DOS), we can define the optical joint density of states (OJDS), as [21–23]:

$$J_1(E) = \frac{2E\varepsilon_2(E)}{\pi E_p^2} \tag{3}$$

where E_p is the plasmon energy in Drude model:

$$E_p^2 = \frac{\hbar^2 n e^2}{\varepsilon_0 m} \tag{4}$$

Here *n* is the total charge density, *e* the electron charge, *m* the mass of the electron and ε_0 is the permittivity of vacuum.

Experimental

The alloy was prepared by the fusion of pure elements (99.99%) in an induction furnace, and a single crystalwas growth by a modified Bridgman method. The single crystalwas oriented by the X-ray back Laue method with its normal axis lying very close to the [0 0 1] direction. Thin specimens suitable for electron microscopy were prepared by a double jet electrochemical thinning.

Electron energy loss spectroscopy (EELS) was used to study the transitions from disordered austenite to ordered austenite to martensite by measuring the changes in electronic structure of element copper in a single crystal of Cu–11.25 wt%Al–0.5 wt%Be alloy, oriented in the [0 0 1] direction, in both the low energy loss (<50 eV) and high

energy loss (>50 eV) regions, in an in-situ cooling process at 500, 200 and 20 °C temperatures.

Transition temperature for order–disorder was about 450 °C as determined by differential scanning calorimetry (DSC), and the martensitic transformation occurred at about 100 °C.

Electron energy loss spectra were obtained using a Gatan Parallel Electron Energy Loss Spectrometer (PEELS model 766) attached to a Philips CM-200 transmission electron microscope (TEM). Spectra were taken in diffraction mode with 0.1 and 0.3 eV/ch dispersion, an aperture of 3mmand a collection semiangle of 10 mrad. The resolution of the spectra was determined by measuring the full width at half-maximum (FWHM) of the zero-loss peak and this was typically close to 1.0 eV for the low energy region where a 0.1 eV/ch dispersion was used and 1.5 eV for the high energy region for a 0.3 eV/ch dispersion, when the TEM was operated at 200 kV.

The EELS spectra were corrected for dark current and readout noise. The channel to channel gain variation was minimized by normalizing the experimental spectrum with independently obtained gain spectrum of the spectrometer. All spectra were examined for oxygen edges to prevent any surface oxides.

Spectra in the high energy region were backgroundsubtracted by fitting the pre-edge backgrounds with a power-law function and then Fourier-ratio deconvoluted to remove multiple scattering components from the spectra. In the low energy region, spectra were Fourier-log deconvoluted to obtain single scattering distributions S(E).

Several spectra were obtained from three different samples and at least two regions in every sample.

Results and discussion

Figs. 1 and 2 show micrographs and diffraction patterns of the alloy at 200 °C (ordered austenite) and room temperature (martensite), respectively. It is clearly observed, from twin boundaries in the bright field micrographs and streaks in the diffraction patterns, that a martensitic transformation has taken place.

Fig. 3 shows energy loss spectra for Cu L_{23} ionization edges for disordered austenite (A2), ordered austenite (DO_3) and martensite (18R), where spectra were shifted up for clarity. After background-subtracted and Fourier-ratio deconvoluted, spectra were aligned so that the value of the threshold energy, measured at one-tenth of the half-height of the L_3 white line,was at 931 eV. We did not attempt to measure chemical shifts of the absorption edges due to these transitions as they are very small (within the experimental resolution).

To extract the white lines we closely follow the empirical method developed by Pearson et al. [14], by modeling the background with a double step function, with steps at L_2 and L_3 peaks. A step line was fit to the background immediately following the L_2 white line. This line was then modified into a double step of the same slope with onsets occurring at the white lines maxima. The ratio of the step heights was chosen as 2:1 which is the multiplicity of the initial steps (four $2p_{3/2}$ electrons and two $2p_{1/2}$ electrons). The white lines area was then divided by the area in a normalization window50 eVin

width, beginning 50 eV past the onset of the L_3 white line, which yields a normalized white-line intensity for the alloy.

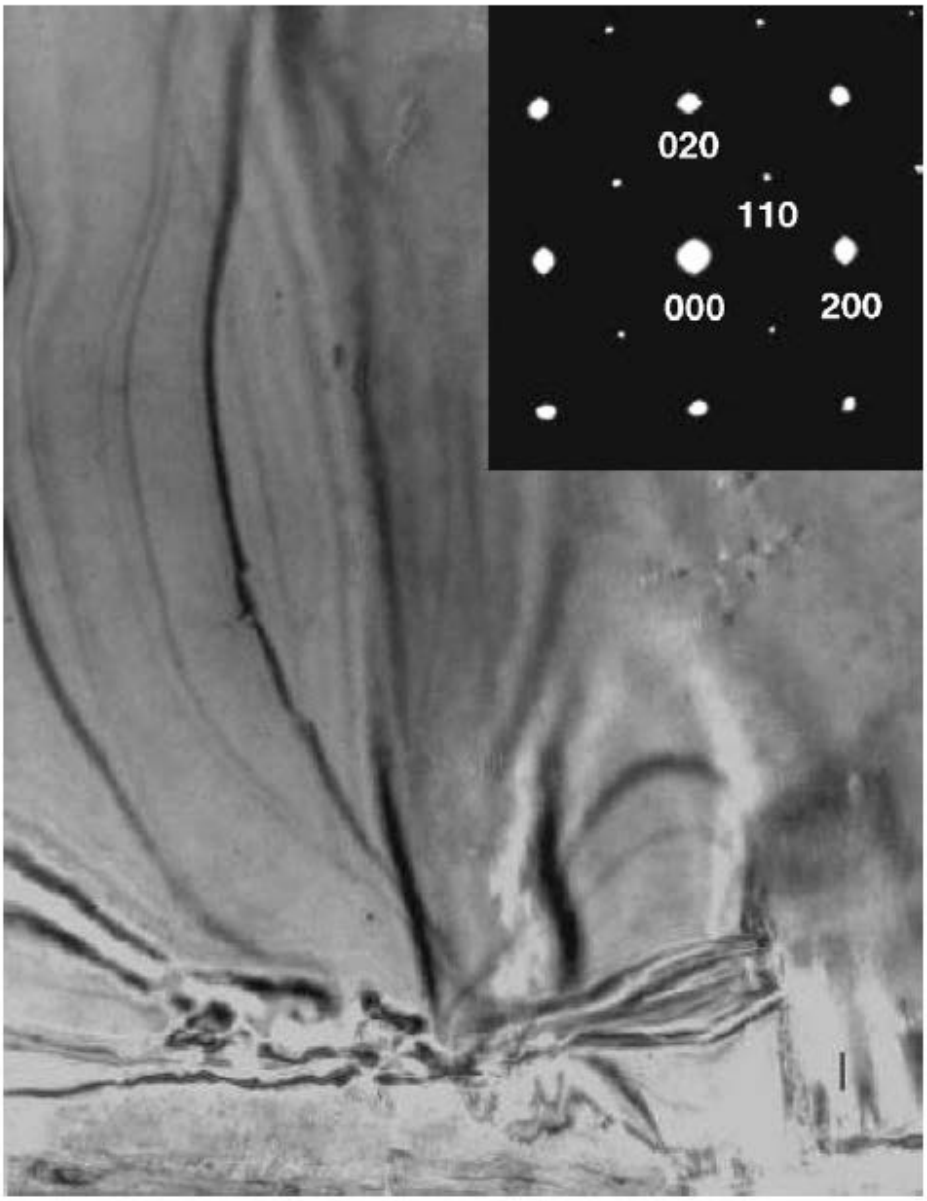

Fig. 1. Micrograph and diffraction pattern for DO_3 structure (ordered austenite) at 200 °C.

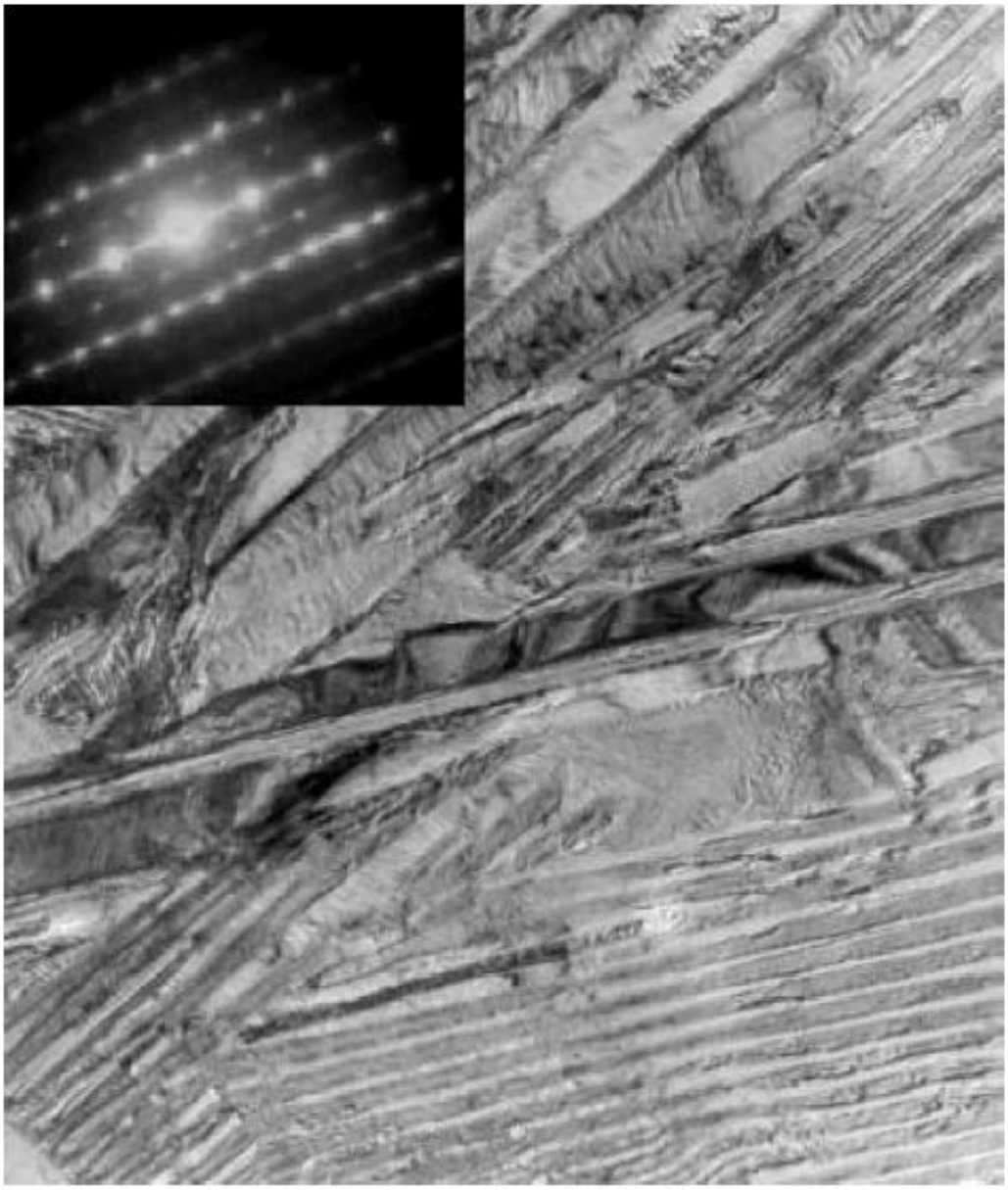

Fig. 2. Micrograph and diffraction pattern for 18R structure (martensite) at 20 °C.

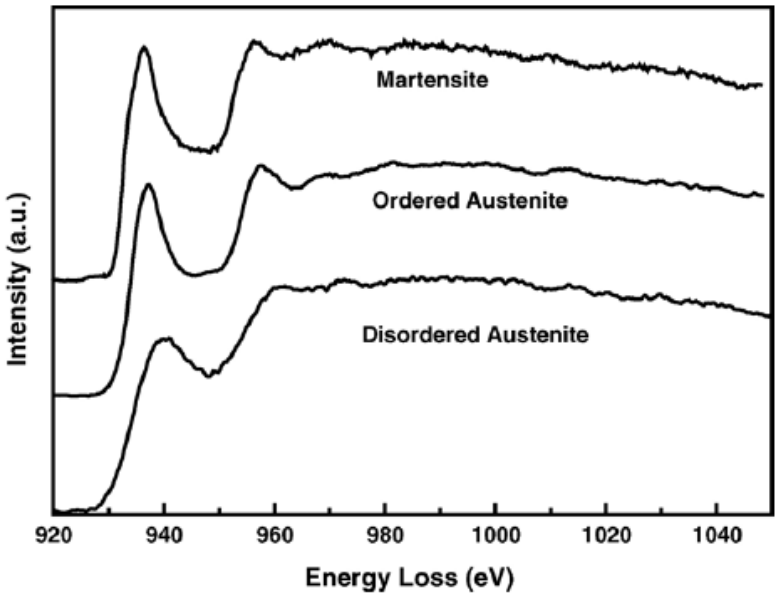

Fig. 3. Superposition of Cu $L_{2,3}$ edges from A2 (disordred austenite), DO_3 (ordered austenite) and 18R (martensite) structures.

Following the above steps is important if we want to use the linear relationship between normalized L_2 and L_3 areas and 3d occupation number, derived by Pearson et al. [12–14]. Dividing by the matrix-element factor, that is 0.172 for copper, and using Eq. (1) allows us to obtain Δn_{3d} in electrons/atom for the transitions.

Fig. 4 illustrates the procedure outlined above and the double step fit to L_{23} white lines for Cu in the A2-structure (disordered austenite). The area under the spectrum and above the double step is associated to the white lines. We can also obtain the ratio L3/L2 whose variation is related to the valence sates, although the relation is not linear. Table 1 shows results obtained for the three states of the alloy.

From Table 1 it is observed that no charge transfer occurs during order–disorder transition, as the measured value (0.02 electrons/atom) is less than Pearson's associated uncertainty (0.06 electrons/atom). On the other hand, during martensitic

transformation, when going from ordered austenite to martensite, copper gains 0.17 electrons/atom. As mentioned above, spectra were acquired from three different samples and at least two regions in every sample and the statistical uncertainty was ~0.02 electrons/atom.

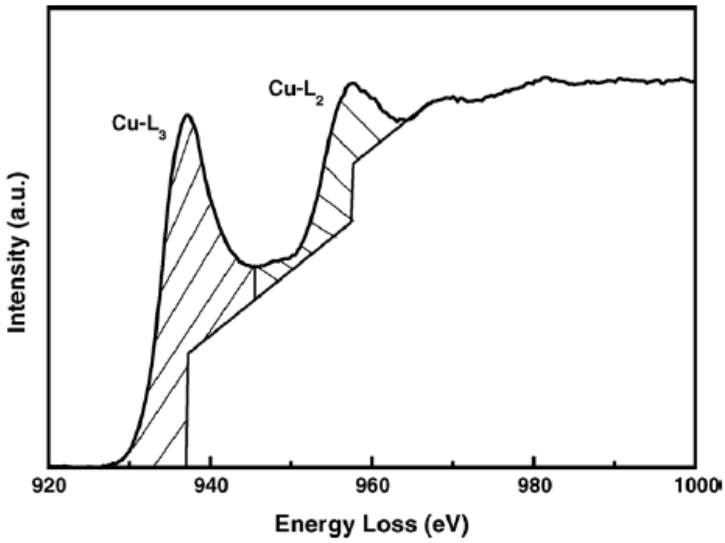

Fig. 4. An EELS spectrum acquired from disordered austenite, showing the technique used to extract the intensity of white lines (hatched area).

Table 1
Results obtained for the white lines ratio and 3d electron occupancy

Structure	L_3/L_2	L_{23}	n_{3d}
A2	2.47	0.171	9.08
DO_3	2.88	0.167	9.10
18R	3.75	0.135	9.27

It is generally believed that changes in the local electronic structure are the result of local compositional and structural differences, being the chemical effect superior over the structural one. In martensitic transformation, which is a diffusionless process, no appreciable changes would be expected in the electronic structure due to chemical

changes. However, during the order–disorder transition, which is a diffusive process we were not able to detect any electronic migration but it occurred during martensitic transformation. These results imply that the structural changes associated with the martensitic transformation are responsible for the measured difference in the Cu white-line intensities between the two phases, despite other hybridization effects.

Hybridization effects can be best observed in the low energy loss region. Figs. 5–7 show the energy loss function and the Kramers–Kronig derived real and imaginary parts of the dielectric function for A2, DO3 and 18R structures, respectively. The dominant feature in the energy loss spectra is the volume plasmon, complicated by interband transitions, as expected for the noble metals [6]. A close inspection of the energy loss functions shows the presence of a well-defined maximum at 19.3 eV and a shoulder ~17 eV in disordered austenite. For ordered austenite the plasmon shows more structure, being three well-defined maxima at 16.5, 19.1 and 20.5 eV and for martensite a peak at 17.7 eV has appeared and a shoulder now to the right, at~19 eV. These differences are a confirmation that some changes in the electronic structure have taken place during the transformations.

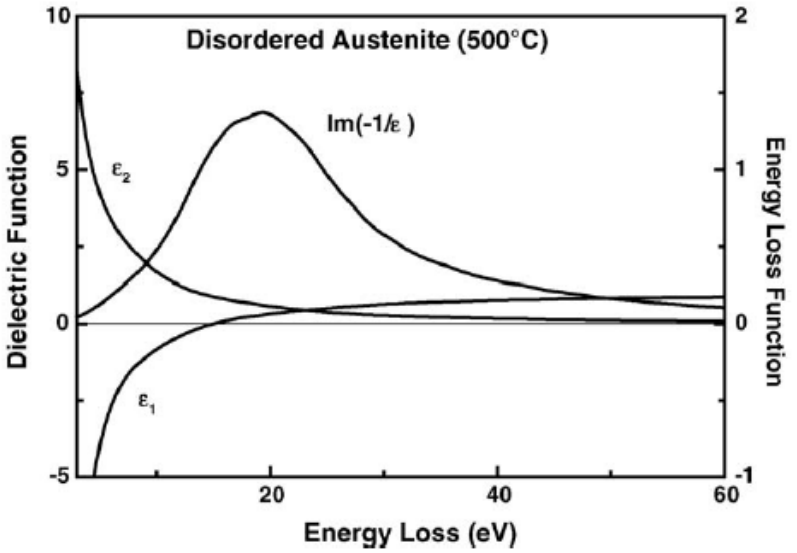

Fig. 5. Energy loss function $\mathrm{Im}(-1/\varepsilon)$, and real and imaginary parts of the dielectric function ε_1, ε_2 for disordered austenite (A2) at 500 °C.

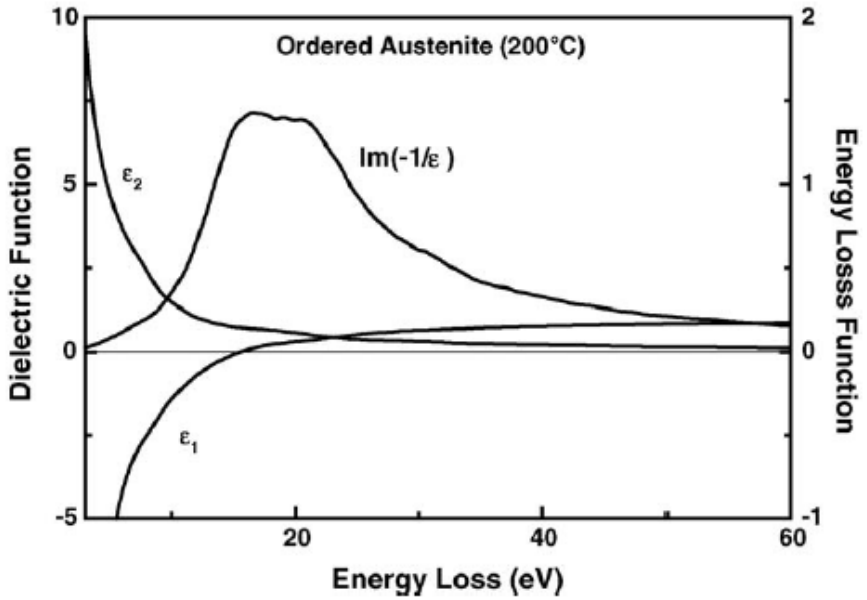

Fig. 6. Energy loss function $\mathrm{Im}(-1/\varepsilon)$, and real and imaginary parts of the dielectric function ε_1, ε_2 for ordered austenite (DO_3) at 200 °C.

As is well known, the plasmon peak position is shifted upward due to excitations below the plasma frequency and downward due to higher energy excitations, so the energy loss spectrum cannot be directly associated with interband transitions. However, as the imaginary part of the dielectric function can be directly associated with interband transitions we should be able to relate these transitions with peaks in the ε2 spectra. Even though it is difficult to see such structure directly from the ε2 versus E curves, it is still possible to enhance these peaks by plotting the optical joint density of states (J_1), defined in Eq. (3). Fig. 8 shows J1(E) for the three structures. It is noted that some peaks associated with interband transitions have been enhanced. Taking the second derivative of $J_1(E)$ with respect to E, peaks not visible in the $J_1(E)$ versus E plots show relative maxima in $-d^2J_1(E)/dE^2$ versus E plots. A close inspection of these curves, shown in Fig. 9, shows that peak positions are different in three structures, being DO_3 structure the one that shows more structure.

Wiggles in the second derivative of the OJDS have no physical meaning but are just a mathematical procedure to enhance the structure not visible, at first sight, in the OJDS versus *E* plot.

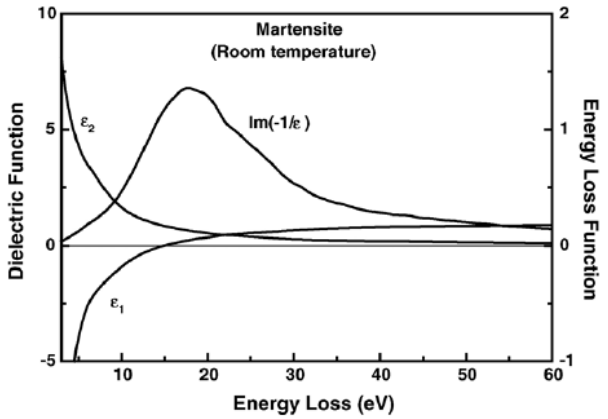

Fig. 7. Energy loss function Im(−1/ε), and real and imaginary parts of the dielectric function ε_1, ε_2 for martensite (18R) at room temperature.

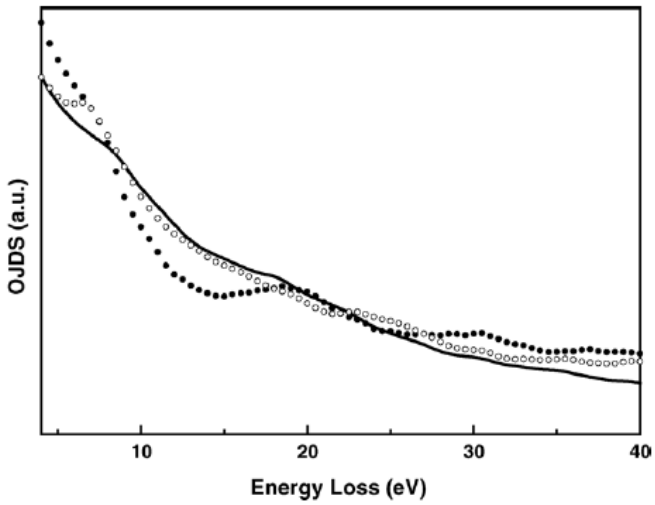

Fig. 8. Kramers–Kronig derived optical joint density of states $J_1(E)$, for disordered austenite (—), ordered austenite (●) and martensite (○) structures.

However, peak positions in the derivative correspond with peaks positions in OJDS. Now, assuming the oscillator strength for a transition from an occupied state in a band to an unoccupied state in other band is frequency-independent, the OJDS is proportional to the joint density of states (JDOS) [22]. The electronic structure information available in the low loss EELS spectrum is related to the joint density of states which is high for energies at which two energy surfaces lie parallel to one another at a particular k point in reciprocal space. At such points one has the so-called critical points. As single electron interband transitions depend on critical points in the band structure, peaks in the imaginary part of the dielectric function give rise to the presence of critical points in the band structure. As peak positions in A2, DO_3 and 18R are all different, as seen in the second derivative curves, we conclude that energy band structure and therefore the density of states have changed when going from disordered austenite to ordered austenite to martensite. Unfortunately, we have not been able to

find energy band structure calculations for this alloy, from where we could give some more insight into the origins of the effects presented.

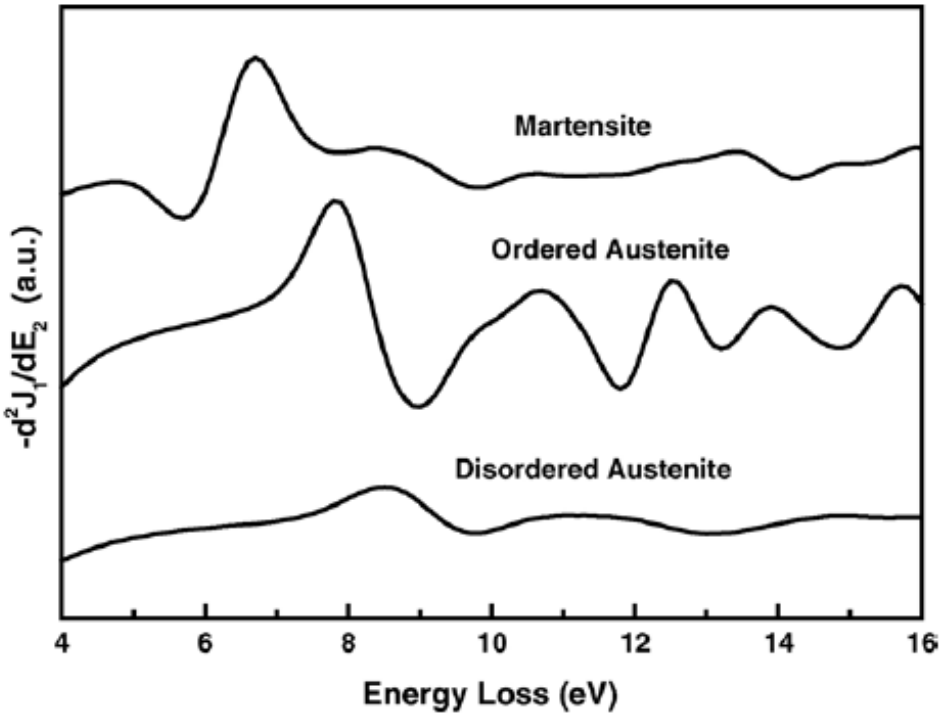

Fig. 9. Second derivative of the optical joint density of states for disordered austenite (A2), ordered austenite (DO_3) and martensite (18R) structures.

Conclusions

Changes in the electronic structure during order–disorder and martensitic transformations in a Cu–Al–Be alloy were studied by electron energy loss spectroscopy, by analyzing the changes in Cu $L_{2,3}$ white-line intensity in A2 (disordered austenite), DO_3 (ordered austenite) and 18R (martensite) structures. It was found that about 0.17 electrons/atom left Cu 3d states after the martensitic transformation, when going from martensite to austenite and no charge transfer is observed during order–disorder transition. An analysis in the low loss region shows that a rearrangement in the energy

band structure of the alloy takes place during both transformations. Even though changes in low loss spectra are small, the technique might be used to monitor similar crystallographic changes in other materials.

References

[1] International Conference On Martensitic Transformations (ICOMAT-95), J. Phys. IV, Vol. 5, Colloque C8, 1995.

[2] International Conference On Martensitic Transformations (ICOMAT-98), Mater. Sci. Eng. A, 1999 (Special Issue).

[3] M. Jurado, T. Castan, L. Ma˜nosa, A. Planes, J. Bassas, X. Alcob´e, M. Morin, Philos. Mag. A 75 (1997) 1237.

[4] H. Warlimont, L. Delaey, Progr. Mater. Sci. 18 (1974) 25.

[5] R.F. Egerton, Electron Energy Loss Spectroscopy in the Electron Microscope, second ed., Plenum Press, New York, 1996.

[6] M.M. Disko, C.C. Ahn, B. Fultz (Eds.), Transmission Electron Energy Loss Spectrometry in Materials Science, The Minerals, Metals and Materials Society, Warrendale, Pennsylvania, 1992.

[7] G. Soto, E.C. Samano, R. Machorro, M.H. Far´ıas, L. Cota-Araiza, Appl. Surf. Sci. 183 (2001) 246.

[8] K. van Benthem, C. Els¨asser, J. Appl. Phys. 90 (2001) 6156.

[9] K. van Benthem, R.H. French, W. Sigle, C. Els¨asser, M. R¨uhle, Ultramicroscopy 86 (2001) 303.

[10] G. Brockt, H. Lakner, Micron 31 (2000) 435.

[11] S.M. Bose, Phys. Rev. Lett. A 289 (2001) 255.

[12] D.H. Pearson, B. Fultz, C.C. Ahn, Appl. Phys. Lett. 53 (1988) 1405.

[13] D.H. Pearson, C.C. Ahn, B. Fultz, Phys. Rev. B 47 (1993) 8471.

[14] D.H. Pearson, C.C. Ahn, B. Fultz, Phys. Rev. B 50 (1994) 12969.

[15] G.Y. Yang, Zhu Jing, J. Magn. Magn. Mater. 220 (2000) 65.

[16] P.L. Potapov, S.E. Kulkova, D. Schryvers, J. Verbeeck, Phys. Rev. 64 (2001) 184110.

[17] G.A. Botton, G.Y. Guo, W.M. Temnerman, C.J. Humphreys, Phys. Rev. B 54 (1996) 1682.

[18] Y. Murakami, D. Shindo, K. Otsuka, T. Oikawa, J. Electron Microsc. 47 (1998) 301.

[19] R.D. Leapman, L.A. Grunes, P.L. Fejes, Phys. Rev. B 26 (1982) 614.

[20] T.G. Sparrow, B.G. Williams, C.N.R. Rao, J.M. Thomas, Chem. Phys. Lett. 108 (1984) 547.

[21] J. Pfl¨uger, J. Fink, W. Weber, K.P. Bohnem, G. Crecelins, Phys. Rev. B 30 (1984) 1155.

[22] W.Y. Liang, A.R. Beal, J. Phys. C 9 (1976) 2823.

[23] F. Espinosa-Maga˜na, A. Duarte-Moller, R. Mart´ınez-S´anchez, M. Miki-Yoshida, J. Electron Spectrosc. Relat. Phenom. 125 (2002) 119.